

**A METHOD FOR RESOLVING THE LASER INDUCED
LOCAL HEATING OF MOVING MAGNETO-OPTICAL
RECORDING MEDIA**

By

Thomas R. Hoffend Jr.

Peter Smereka

and

Roger J. Anderson

IMA Preprint Series # 891

October 1991

**A METHOD FOR RESOLVING THE
LASER INDUCED LOCAL HEATING OF
MOVING MAGNETO-OPTICAL RECORDING MEDIA**

by

Thomas R. Hoffend Jr.,*

Peter Smereka,**

and

Roger J. Anderson†

Introduction

Local heating of thin multi-layer structures by a scanning laser beam plays a fundamental role in many technologies. We are primarily interested in magneto-optical (MO) recording, which is accomplished by heating a magnetic thin film embedded in a stack of layers of varying thicknesses and material properties (Fig. 1) with a tightly focused laser beam. In this paper we describe a method for resolving to first order the heating of such a configuration, assuming certain geometries peculiar to typical MO disks.

Numerous procedures for calculating the laser heating of layered structures have appeared. Exemplary general purpose techniques for the full linear problem employ alternating direction implicit schemes^{1,2} spectral methods³ or finite

* Institute for Mathematics and its Applications, University of Minnesota, 206 Church Street S.E., Minneapolis, MN 55455.

** Currently at Dept. of Mathematics, UCLA, Los Angeles, CA 90024-1555.

† 3M Company, Bldg. 201-1C-18, 3M Center, St. Paul, MN 55144.

element methods. The full implementation of these, requiring large number of gridpoints or elements and long computation times, are cumbersome in nature. Some highly simplified techniques have also been found useful in determining the character of the temperature profile, but only for single stationary laser pulses of very short duration.^{4,5} The goal of this work is to bridge the gap. We thus present a model of intermediate computational complexity that includes sufficient physics to qualitatively exhibit the nature of the solution of the full linear problem and that remains valid for all time intervals.

The work is divided into five sections. We provide a description of the physical system under consideration and then develop a model which is applicable to typical MO disk stacks. Analysis of the new model yields a single integro-differential equation for the temperature distribution in the MO layer. A fast solution technique for the governing integro-differential equation immediately follows. We conclude with a presentation of some numerical results and a comparison of these results with those obtained using an algorithm based on an alternating direction implicit scheme.

I. Description of the Physical System

In Fig. 1 we diagram a cross-section of an “ideal” MO disk stack. The stack consists of $N + 2$ layers of varying thickness l_i (m), thermal conductivity k_i (W/mK), density ρ_i (kg/m³), heat capacity C_i (J/kgK), and complex index of refraction n_i . We assume that the material properties are temperature independent over the range of temperatures reached in MO recording. Layers zero ($i = 0$) and $i = N + 1$ represent the substrate and superstrate, respectively. We remark that the picture is not drawn to scale in that the thicknesses l_0 and l_{N+1} are typically of the order of a millimeter, while the net thickness

$$l \stackrel{\text{def}}{=} \sum_{i=1}^N l_i \quad (1)$$

of the central or *active region* is typically of the order of two tenths of a micron. We further allow that the disk extends uniformly and infinitely in the xy plane.

A scanning laser beam, assumed to have a Gaussian intensity profile with intensity I (W/m²) and spot size r_0 (m), illuminates the disk at normal incidence to the surface and moves with constant velocity v in the positive x -direction. The laser is turned on at time $t = 0$ and modulated by a time function $p(t)$. The intensity $I_0(x, y, t)$ incident at the surface can thus be written

$$I_0(x, y, t) = I p(t) \exp\{-[(x - vt)^2 + y^2]/r_0^2\}, \quad (2)$$

where I denotes the average intensity of the laser beam. For a single pulse of duration t_0 , the function $p(t)$ takes the form

$$p(t) = u(t)u(t_0 - t), \quad (3)$$

where $u(t)$ is the unit step function.

As noted in Ref. 3, the process of calculating the temperature rise due to absorption of the laser beam by the stack separates nicely into an optics problem followed by a heat conduction problem. In the optics problem one determines the rate of absorption of laser power and conversion to heat as a function of position in the stack. In the thermal problem one calculates the evolution of the objects temperature as driven by the rate of heat generation found in the first problem.

We follow Refs. 1 and 3 in modeling the incident laser beam as a normally incident plane wave with surface intensity profile given by the relation (2). A detailed solution of the optics problem can be found in Ref. 6. It turns out that under the simplifying assumptions outlined in section II, we will only require the percent total incident power absorbed by each layer. Solution of the heat conduction problem remains our primary concern.

II. A New Model for Magneto-optical Disks

We obtain the simplest tractable physical system exhibiting the general behavior of a MO disk stack by assuming that the active region is covered on both sides with (possibly different) insulating materials extending to infinity in the $\pm z$ directions. The relative thickness of the substrate and superstrate compared to

the net thickness of the middle region validates this assumption. The multilayer extends uniformly and indefinitely in the xy plane. This geometry corresponds to that of Fig. 1 with the thicknesses l_0 and l_{N+1} set to infinity.

Heat is generated by a laser beam with intensity profile as discussed in section I. The materials comprising the substrate and the superstrate are assumed to have purely real indices of refraction, i.e. they do not absorb any of the laser light, and thus all heat generation takes place in the active region. We note that even though the active region consists of several layers, its net thickness l remains very small. Second, the temperature rise across the thickness of the active region, though certainly non-constant, has a highly non-trivial average value. Also, the variation of the temperature in the active region is greatest across the non-conducting spacer layers. Since these layers are generally thin compared to the net thickness l , the contribution to any deviation from the average temperature rise across the net thickness will be small. Furthermore, we can consider that l is so small that the radial diffusion distance reached in the middle layer and the distance travelled along the surface by the laser in the time it takes to achieve uniform temperature across the thickness of the layer is negligible compared to the spot size of the laser. Diffusion into the substrates and superstrates is also negligible during this time. We therefore make the fundamental simplifying assumptions that the rate of transfer of optical to heat energy is immediate and uniform across the thickness of the active region and that the temperature rise in the active region is predominantly determined by its average value, and as a first order approximation, we can take it to be uniform across the thickness. Continuity of the temperature and the heat flux at the interfaces internal to the active region is then identically satisfied. If we take the aluminum reflector to be moderately thin so as to avoid sinking all of the heat away from the MO layer, the average temperature rise across the thickness of the active region is a good indication of the temperature rise across the thickness of the MO layer. We therefore consider only the radial (with the radius $r^2 = x^2 + y^2$) diffusion in the active region, treating it in some sense like a single thin layer.

Due to the assumed uniformity of heat generation across the active region, we can express the rate of supply of energy to this area as

$$g(x, y, t) = A^* I_0(x, y, t), \quad (4)$$

where A^* is the percentage of the total laser power absorbed by the entire active region. We denote the temperature rise of the active region T_a .

By considering the balance of power in an arbitrary test volume and using continuity of the temperature flux across the interfaces between the active region and the substrate and superstrate, one can readily show that under our fundamental simplifying assumptions the equation of heat conduction in the active region takes the form

$$l\rho^*C^*\frac{\partial T_a}{\partial t} = k^*l^*\nabla_{\perp}^2 T_a + k_{N+1}\frac{\partial T_{N+1}}{\partial z}\Big|_{z=l/2} - k_0\frac{\partial T_0}{\partial z}\Big|_{z=-l/2} + g, \quad (5)$$

where

$$\nabla_{\perp}^2 \stackrel{\text{def}}{=} \frac{\partial^2}{\partial x^2} + \frac{\partial^2}{\partial y^2}, \quad (6)$$

$$l = \sum_{i=1}^N l_i, \quad (7)$$

$$\rho^*C^* = \sum_{i=1}^N \frac{l_i}{l} \rho_i C_i, \quad (8)$$

$$k^* = \sum_{i=1}^N \frac{l_i}{l} k_i. \quad (9)$$

The corresponding equations for the other two layers are

$$\rho_i C_i \frac{\partial T_i}{\partial t} = k_i \left(\nabla_{\perp}^2 + \frac{\partial^2}{\partial z^2} \right) T_i, \quad i = 0 \text{ and } i = N + 1. \quad (10)$$

We also have the continuity conditions

$$T_0|_{z=-l/2} = T_a|_{z=-l/2}, \quad (11a)$$

$$T_2|_{z=l/2} = T_a|_{z=l/2}, \quad (11b)$$

and the initial conditions

$$T_a|_{t=0} = 0, \quad (12a)$$

$$T_i|_{t=0} = 0, \quad i = 0, N + 1. \quad (12b)$$

The equations (5) and (10) form a coupled system of partial differential equations. We wish to solve these equations, together with the continuity conditions (11a,b) and initial conditions (12a,b), for the temperature rise T_a . In the next

section, this coupled system is reduced to a single integro-differential equation for the temperature rise T_a .

III. Governing Integro-Differential Equation for T_a

In order to solve the coupled system of partial differential equations (5) and (10), we first introduce a normalization of the form

$$\xi = \frac{x}{r_0}, \quad \eta = \frac{y}{r_0}, \quad \zeta = \frac{z}{l}, \quad \tau = \frac{\kappa^* t}{l^2}, \quad (13)$$

$$\epsilon = \left(\frac{l}{r_0}\right)^2, \quad \nu = \frac{l^2 \nu}{r_0 \kappa^*}, \quad \lambda = \frac{l}{k^*},$$

and we define

$$\alpha_i = \frac{\kappa_i}{\kappa^*}, \quad \beta_i = \frac{k_i}{k^*}, \quad i = 0 \text{ and } N + 1, \quad (14)$$

where in general the diffusivities κ_i and κ^* are given by the relation $\kappa = k/\rho C$. Equations (5) and (10) can then be written in the form

$$\frac{\partial T_a}{\partial \tau} = \epsilon \nabla^2 T_a + \beta_{N+1} \frac{\partial T_{N+1}}{\partial \zeta} \Big|_{\zeta=1/2} - \beta_0 \frac{\partial T_0}{\partial \zeta} \Big|_{\zeta=-1/2} + \lambda g, \quad (15)$$

$$\frac{\partial T_i}{\partial \tau} = \alpha_i \left(\epsilon \nabla^2 + \frac{\partial^2}{\partial \zeta^2} \right) T_i, \quad i = 0 \text{ and } i = N + 1, \quad (16)$$

with the continuity conditions

$$T_0 \Big|_{\zeta=-1/2} = T_a \Big|_{\zeta=-1/2}, \quad (17a)$$

$$T_2 \Big|_{\zeta=1/2} = T_a \Big|_{\zeta=1/2}, \quad (17b)$$

and the initial conditions

$$T_a \Big|_{\tau=0} = 0, \quad (18a)$$

$$T_i \Big|_{\tau=0} = 0, \quad i = 0 \text{ and } N + 1, \quad (18b)$$

where

$$\nabla^2 \stackrel{\text{def}}{=} \frac{\partial^2}{\partial \xi^2} + \frac{\partial^2}{\partial \eta^2}. \quad (19)$$

We now make one final simplifying assumption. In eqn. (16) typically the parameter $\epsilon \ll 1$, even when we consider that l represents the entire thickness of the active region. We thus consider that in the substrate and superstrate diffusion in the axial (i.e. z) direction dominates radial diffusion and we drop the terms containing ϵ in eqn. (16). Note that our previous assumptions made in the derivation of the governing equation for the temperature rise T_a in the active region say just the opposite, i.e. in the active region diffusion in the radial direction dominates and axial diffusion only enters in terms involving heat lost to the substrate and superstrate. Equation (16) thus takes the form

$$\frac{\partial T_i}{\partial \tau} = \alpha_i \frac{\partial^2 T_i}{\partial \zeta^2}, \quad i = 0 \text{ and } i = N + 1. \quad (20)$$

By applying Duhamel's principle, the temperature gradients at $\zeta = \pm 1/2$ are readily found to be

$$\left. \frac{\partial T_i}{\partial \zeta} \right|_{\zeta=\pm 1/2} = \mp \frac{1}{\sqrt{\pi \alpha_i}} \int_0^\tau \frac{\partial T_a(\xi, \eta, \tau')}{\partial \tau'} \frac{d\tau'}{\sqrt{\tau - \tau'}}. \quad (21)$$

We now substitute the result (21) in eqn. (15) and collect terms. This results in a single integro-differential equation for the temperature rise T_a

$$\frac{\partial T_a}{\partial \tau} = \epsilon \nabla^2 T_a - \frac{P_0}{\sqrt{\pi}} \int_0^\tau \frac{\dot{T}_a(\xi, \eta, \tau')}{\sqrt{\tau - \tau'}} d\tau' + \lambda g, \quad (22)$$

where a dot over a kernel denotes partial differentiation with respect to the parameter τ' , and where

$$P_0 \stackrel{\text{def}}{=} \frac{\beta_1}{\sqrt{\alpha_1}} + \frac{\beta_2}{\sqrt{\alpha_2}}. \quad (23)$$

In the next section we describe a method of solution for eqn. (22).

IV. Solution of the Governing Integro-Differential Equation

Consider eqn. (22)

$$\frac{\partial T_a}{\partial \tau} = \epsilon \nabla^2 T_a - \frac{P_0}{\sqrt{\pi}} \int_0^\tau \frac{\dot{T}_a(\xi, \eta, \tau')}{\sqrt{\tau - \tau'}} d\tau' + \lambda g,$$

for $\tau \geq 0$, where P_0 and ϵ are constants and

$$g(\xi, \eta, \tau) = g_1(\xi - \nu\tau, \eta) p(\tau), \quad (24)$$

where for a single laser pulse turned on at (normalized) time $\tau = 0$ and off at $\tau = \tau_0 = \kappa^* t_0/l^2$ we have

$$p(\tau) = u(\tau) u(\tau_0 - \tau). \quad (25)$$

When the laser beam has a Gaussian intensity profile as described in Section I. we have

$$g_1(\xi, \eta) = \exp\{-(\xi^2 + \eta^2)\}. \quad (26)$$

We remark that even though we have chosen a simple function for $p(\tau)$, the method can be easily generalized to include multiple and/or multi-level pulses.

Taking the (causal) Laplace transform of eqn. (22) with respect to τ and the two-dimensional Fourier transform

$$\widehat{u}(\omega_\xi, \omega_\eta) \stackrel{\text{def}}{=} \int_{-\infty}^{\infty} \int_{-\infty}^{\infty} u(\xi, \eta) \exp\{-i(\xi\omega_\xi + \eta\omega_\eta)\} d\omega_\xi d\omega_\eta,$$

of the same equation with respect to the spacial coordinate variables (ξ, η) we get

$$s \widehat{\overline{T}}_a(\omega_\xi, \omega_\eta, s) = -\epsilon \omega^2 \widehat{\overline{T}}_a - P_0 \sqrt{s} \widehat{\overline{T}}_a + \lambda \widehat{g}, \quad (27)$$

where a bar over a kernel represents Laplace transform, a hat over a kernel represents Fourier transform, and where

$$\omega^2 \stackrel{\text{def}}{=} \omega_\xi^2 + \omega_\eta^2. \quad (28)$$

Solving for $\widehat{\overline{T}}_a$, we get

$$\widehat{\overline{T}}_a(\omega_\xi, \omega_\eta, s) = \frac{\lambda \widehat{g}(\omega_\xi, \omega_\eta, s)}{s + P_0 \sqrt{s} + \epsilon \omega^2} = \lambda \widehat{h}(\omega_\xi, \omega_\eta, s) \widehat{g}(\omega_\xi, \omega_\eta, s), \quad (29)$$

where

$$\widehat{h}(\omega_\xi, \omega_\eta, s) \stackrel{\text{def}}{=} \frac{1}{\sqrt{s}} \left[\frac{\sqrt{s}}{s + P_0 \sqrt{s} + \epsilon \omega^2} \right]. \quad (30)$$

Taking the inverse Laplace transform of eqn. (30) we get

$$\widehat{h}(\tau) = \frac{1}{2} \left[\left(1 - \frac{\alpha}{\beta}\right) w\{i(\alpha - \beta)\sqrt{\tau}\} + \left(1 + \frac{\alpha}{\beta}\right) w\{i(\alpha + \beta)\sqrt{\tau}\} \right], \quad (31)$$

where $w(z)$ is the standard analytic function⁷

$$w(z) = e^{-z^2} \operatorname{erfc}(-iz), \quad (32)$$

where $\operatorname{erfc}(z)$ is the complementary error function⁷, and where $\alpha \stackrel{\text{def}}{=} P_0/2$ and $\beta^2(\omega) \stackrel{\text{def}}{=} \alpha^2 - \epsilon\omega^2$. A straightforward application of the power series expansion for $w(z)$ yields the result that $\hat{h}(\tau)$ is a continuous function of $(\omega_\xi, \omega_\eta)$.

Using eqn. (31), it is now possible to write

$$\hat{T}_a(\tau, \omega_\xi, \omega_\eta) = \lambda \hat{h}(\tau) * \hat{g}(\tau), \quad (33)$$

where it is tacitly understood that we take the convolution with respect to the parameter τ . Due to the nature of $g(\tau, \xi, \eta)$, \hat{g} takes the form

$$\hat{g}(\omega_\xi, \omega_\eta, \tau) = p(\tau) e^{-i\nu\omega_\xi\tau} \hat{g}_1(\omega_\xi, \omega_\eta), \quad (34)$$

where

$$\hat{g}_1(\omega_\xi, \omega_\eta) = \frac{\pi}{4} \exp\{-(\omega_\xi^2 + \omega_\eta^2)/4\}. \quad (35)$$

For a single laser pulse, eqn. (33) can thus be written as

$$\hat{T}_a(\tau) = \lambda \hat{g}_1 \int_0^\infty u(\tau_0 - \tau - \tau') u(\tau - \tau') e^{-i\nu\omega_\xi(\tau - \tau')} \hat{h}(\tau') d\tau'$$

and by virtue of the factor $u(\tau_0 - \tau - \tau') u(\tau - \tau')$ this integral takes the form

$$\hat{T}_a = \lambda \hat{g}_1 e^{-i\nu\omega_\xi\tau} \int_a^b e^{i\nu\omega_\xi\tau'} \hat{h}(\tau') d\tau', \quad (36)$$

where

$$a = a(\tau) = \begin{cases} (\tau - \tau_0), & \text{if } \tau \geq \tau_0; \\ 0, & \text{if } \tau < \tau_0, \end{cases} \quad (37)$$

and

$$b = b(\tau) = \tau. \quad (38)$$

Upon evaluation of the integral in (36) we achieve the result

$$\hat{T}_a(\tau) = \frac{\lambda}{2} \hat{g}_1 e^{-i\nu\omega_\xi\tau} \left[\left(1 + \frac{\alpha}{\beta}\right) I_+ + \left(1 - \frac{\alpha}{\beta}\right) I_- \right], \quad (39)$$

where

$$I_{\pm} = I_{1\pm} + I_{2\pm}, \quad (40)$$

where

$$I_{1\pm} = \frac{(\alpha \pm \beta)}{c_{\pm} \sqrt{\nu \omega_{\xi}}} e^{i\pi/4} \left[\operatorname{erfc} \left\{ e^{-i\pi/4} \sqrt{a\nu\omega_{\xi}} \right\} - \operatorname{erfc} \left\{ e^{-i\pi/4} \sqrt{b\nu\omega_{\xi}} \right\} \right], \quad (41)$$

$$I_{2\pm} = \frac{1}{c_{\pm}} \left[e^{ib\nu\omega_{\xi}} w \{ i(\alpha \pm \beta) \sqrt{b} \} - e^{ia\nu\omega_{\xi}} w \{ i(\alpha \pm \beta) \sqrt{a} \} \right], \quad (42)$$

and

$$c_{\pm} \stackrel{\text{def}}{=} i\nu\omega_{\xi} + (\alpha \pm \beta)^2. \quad (43)$$

By taking appropriate limits one can demonstrate that the apparent singularities in (39) where $\nu = 0$, $\omega_{\xi} = 0$, $\beta = 0$, and/or $c_{\pm} = 0$ are removeable, in other words $\widehat{T}_a(\tau)$ is a continuous function of τ , ω_{ξ} , and ω_{η} . In addition, the properties of \widehat{g}_1 , β , and I_{\pm} indicate that $\widehat{T}_a(\tau)$ decays rapidly as a function of ω_{ξ} and ω_{η} .

Numerical computation of the temperature rise T_a at any fixed time thus requires that we calculate the inverse two-dimensional Fourier transform of an explicitly known, well-behaved function. This can be carried out using a standard inverse Fast Fourier Transform (FFT) algorithm. It turns out that filling the FFT matrix dominates the computation time. Efficient and robust algorithms for computing the complex error function are readily available,⁸ and the net computation time for a series of timesteps remains quite reasonable.

V. Numerical Results

In this section we present some numerical results obtained using the method discussed in this paper for three illustrative test disks. We compare the results with those obtained for the same physical system using an established method based on an alternating direction implicit (ADI) scheme and described in Refs. 1 and 2.

In Table 1 we specify appropriate geometrical and physical parameters for each test disk. We remark that in using the ADI based scheme, we follow Refs. 1 and 2 and assign suitably large values (rather than infinity) to l_1 and l_{N+1} .

We further note that for the sake of simplicity in our demonstration, we have rounded some of the material parameter values but maintained the same order of magnitude. Disk 1 is simply a single thin MO layer sandwiched between two nonconducting layers. This configuration evidently conforms to the fundamental physical assumptions made in this paper. Disk 2 is a structure similar to a typical write-once magneto-optical disk and moderately conforms to the same assumptions. Disk 3 represents a contrivance that is supposed to grossly violate the assumptions.

For each disk we assume a scanning speed of 6.0 meters per second and a laser pulse duration of 100 nano-seconds. For the purpose of comparison with the algorithm published in Refs. 1 and 2, the sign of the velocity v must be taken as negative, i.e. the laser beam actually moves in the negative x -direction. We plot $T_a(x, 0, t_0)$ versus x , that is the temperature rise in the MO layer at the laser spot center versus the x -coordinate at the end of the laser pulse. In figs. 2,3, and 4 we compare the results obtained via the new method with those obtained using the ADI based scheme for disks 1, 2, and 3, respectively.

For disk 1, the difference between the resulting plots is very small. We thus expect the new method to succeed beautifully for conducting mono-layer films on non-conducting substrates. For disk 2 we achieve a maximum difference of approximately ten percent of the value obtained using the ADI based scheme. We conclude that the new method should be helpful in resolving the overall peak shape and behavior of the temperature profile. Finally, we achieve an extremely large (and not unexpected) difference between the results for disk 3. The reason for this failing becomes evident if we examine the temperature rise in the aluminum layers for disks 2 and 3.

In figs. 5 and 6 we compare the corresponding temperature rise in the MO and the aluminum layers for disks 2 and 3, respectively, as obtained using the ADI based scheme. For disk 2, the temperature rise of the aluminum layer closely follows that of the MO layer, thus verifying our assumption of uniform temperature variation across the thickness of the active region. We find that for disk 3, however, the temperature rise of the aluminum layer is vastly different than that of the MO layer. We thus confirm the supposition that disk 3 violates our assumptions and feel no remorse over the blatant difference between the two curves in fig. 4.

Conclusion

Under the simplifying but in many cases physically reasonable assumptions that axial diffusion dominates in the substrate and superstrate, while radial diffusion dominates in the active region, the temperature rise in the active region of a laser-heated, moving magneto-optical disk stack is governed by a single integro-differential equation. The problem of solving this equation at any fixed time reduces to the calculation of the inverse two-dimensional Fourier Transform of a complicated but well behaved function. This computation can be implemented numerically using an inverse Fast Fourier Transform algorithm and an established algorithm for computing the complex error function.

Numerical results for MO disk stacks satisfying the basic physical constraints outlined in the theory are in good agreement with those obtained using a standard but computationally intensive technique based on an alternating direction implicit scheme. Computation times for the new method are a fraction of those required for alternating direction implicit scheme. We expect the method to break down when there are thick non-conducting spacer layers and/or a thick aluminum reflector in the active region. In that case the fundamental assumption of uniform temperature across the active region is violated.

The new method has the further advantage of being able to calculate the temperature rise at any given time, say exactly when the laser beam is turned off, without stepping through all of the previous times. This becomes a major convenience, especially for the longer pulse durations associated with pulse width modulation.

- (1) M. Mansuripur, G.A.N. Connell, and J.W. Goodman, Appl. Opt. **21**, 1106 (1982).
- (2) M. Mansuripur and G.A.N. Connell, Appl. Opt. **22**, 666 (1983).
- (3) R.J. Anderson, J. Appl. Phys. **64**, 6639 (1988).
- (4) U.C. Paek and K. Kestenbaum, J. Appl. Phys. **44**, 2260 (1973).
- (5) P. Hansen, J. Appl. Phys. **62**, 216 (1987).
- (6) M. Born and E. Wolf, *Principles of Optics*, 6th Ed. (Pergamon, New York, 1980), p. 51.
- (7) M. Abramowitz and I. Stegun, *Handbook of Mathematical Functions*. (Dover Publications, Inc., New York, 1989), pp. 295-329.
- (8) ACM Trans. on Mathematical Software. **16**, 47 (1990).

Disk	# of Layers ($N + 2$)	Layer Number (r)	l_r (\AA)	$\rho_r C_r$ (J/Kcm)	k_r (W/cmK)
1	3	0	∞	1.5	0.002
		1	200	3.2	0.05
		2	∞	1.5	0.002
2	6	0	∞	1.5	0.002
		1	300	2.7	0.06
		2	200	3.2	0.05
		3	100	2.7	0.06
		4	500	2.7	0.4
		5	∞	1.5	0.002
3	6	0	∞	1.5	0.002
		1	300	2.0	0.015
		2	200	3.2	0.05
		3	500	2.0	0.015
		4	1500	2.7	0.4
		5	∞	1.5	0.002

Table 1

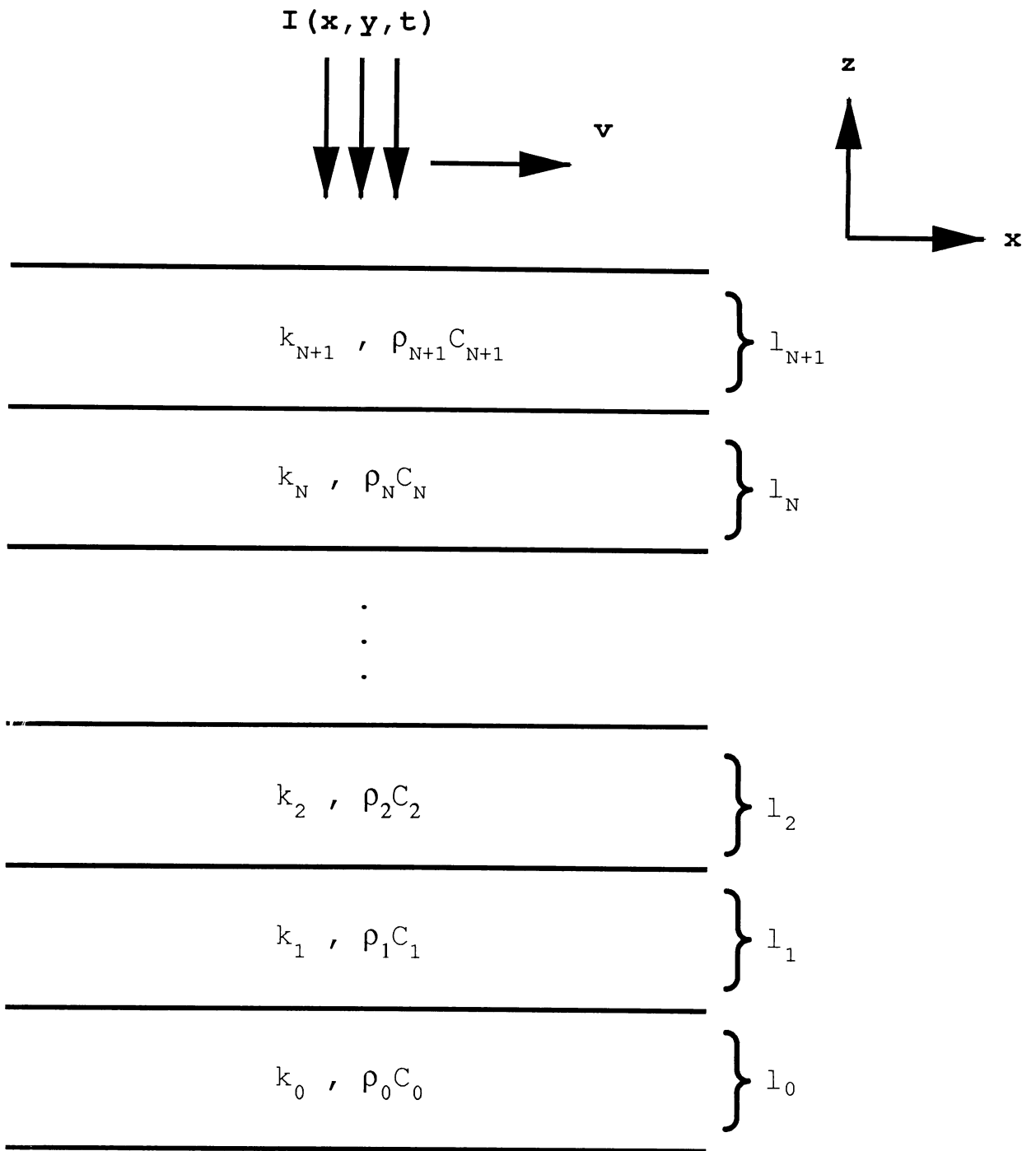


Figure 1

Temperature Rise at Spot Center vs X

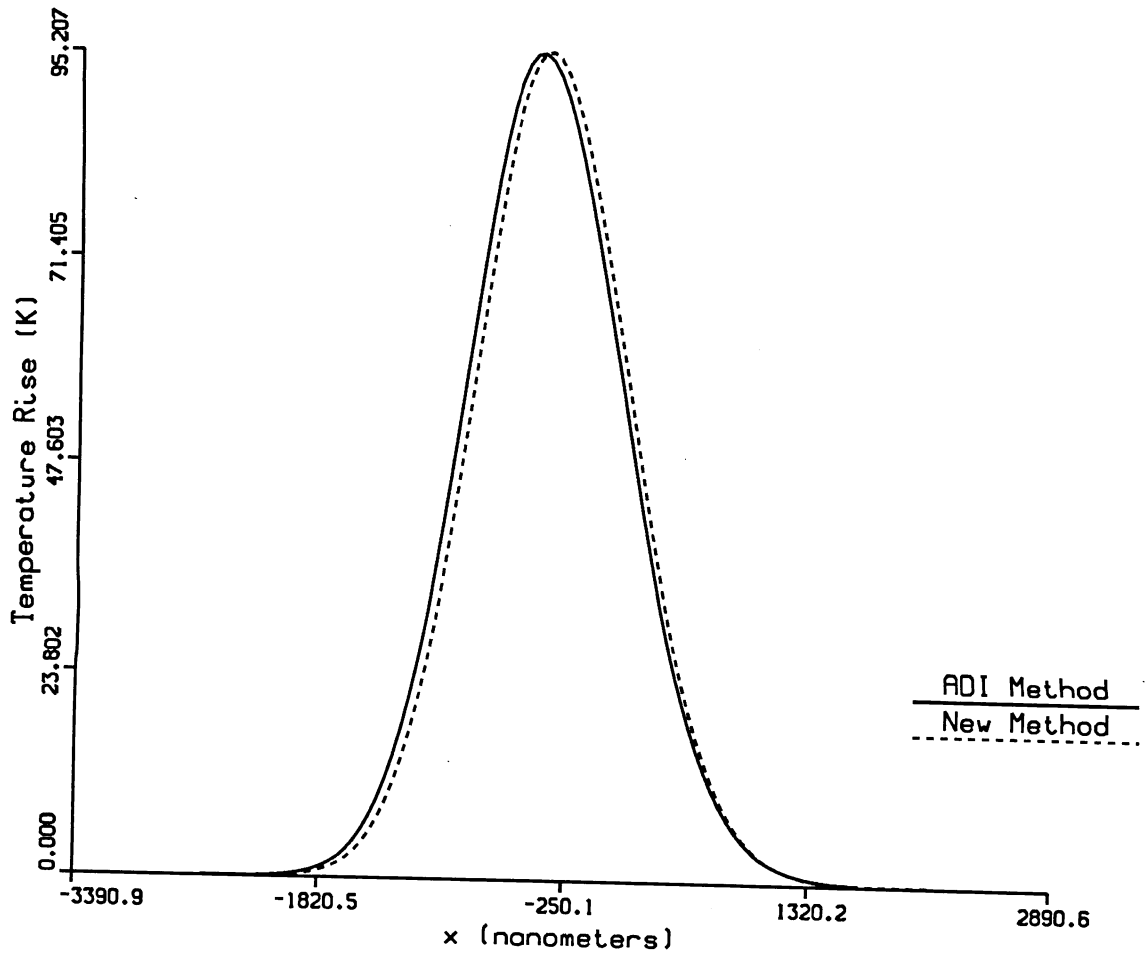


Figure 2

Temperature Rise at Spot Center vs X

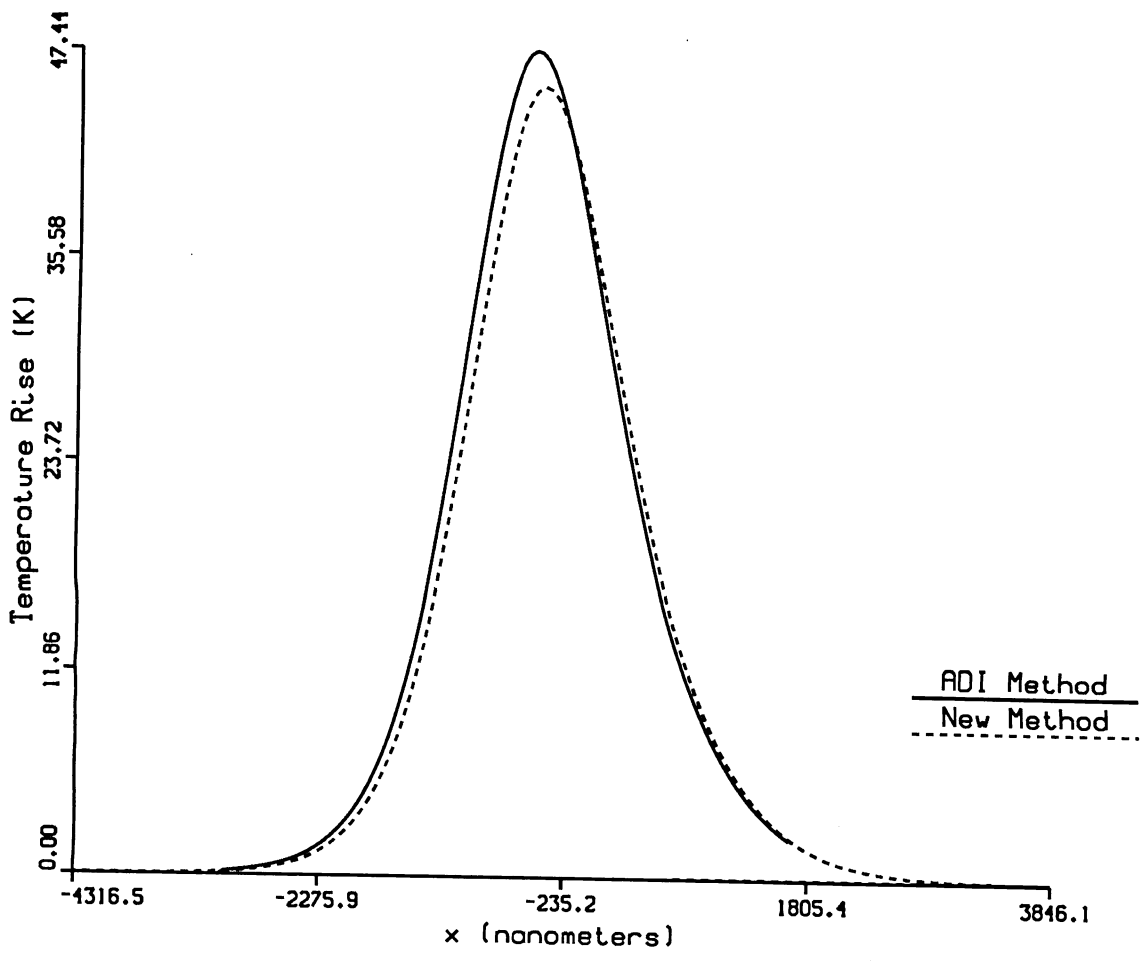


Figure 3

Temperature Rise at Spot Center vs X

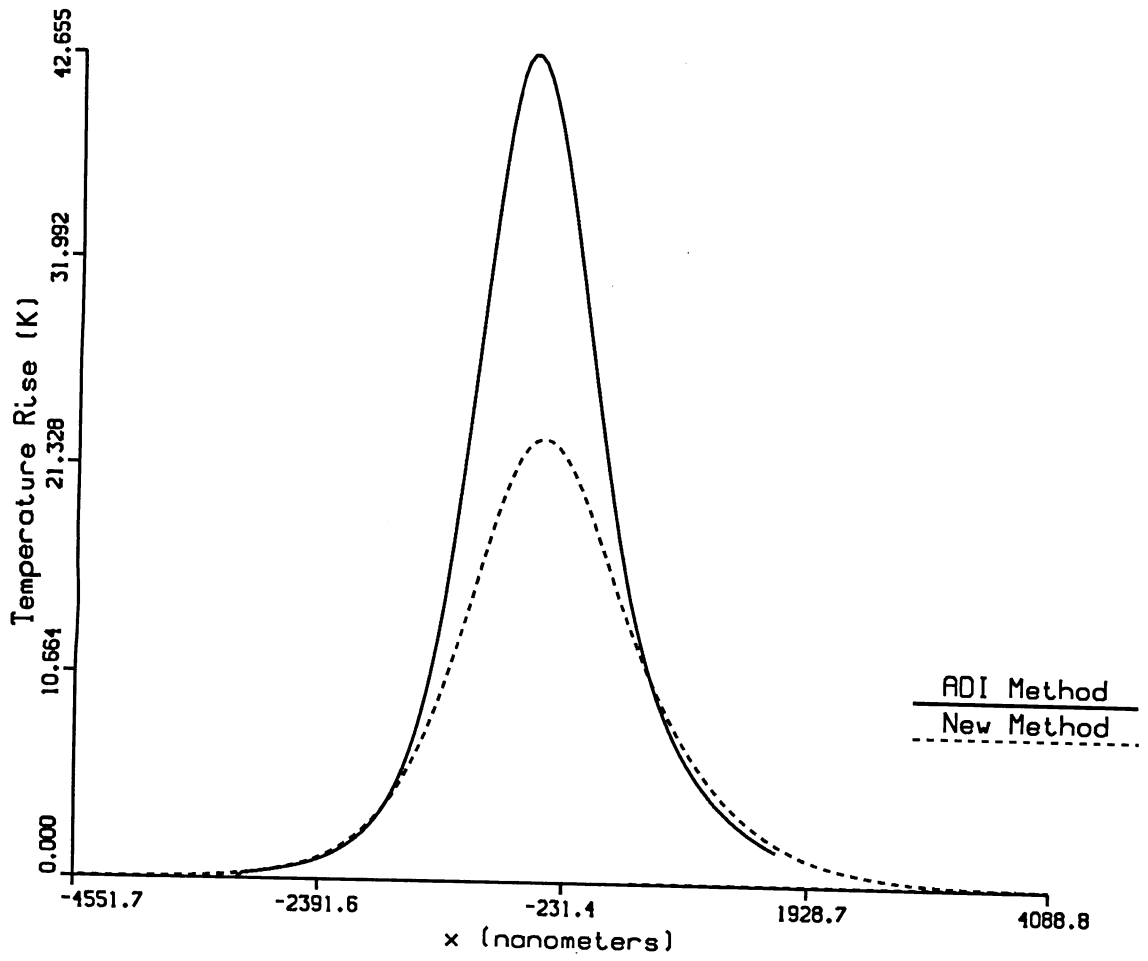


Figure 4

Temperature Rise at Spot Center vs X

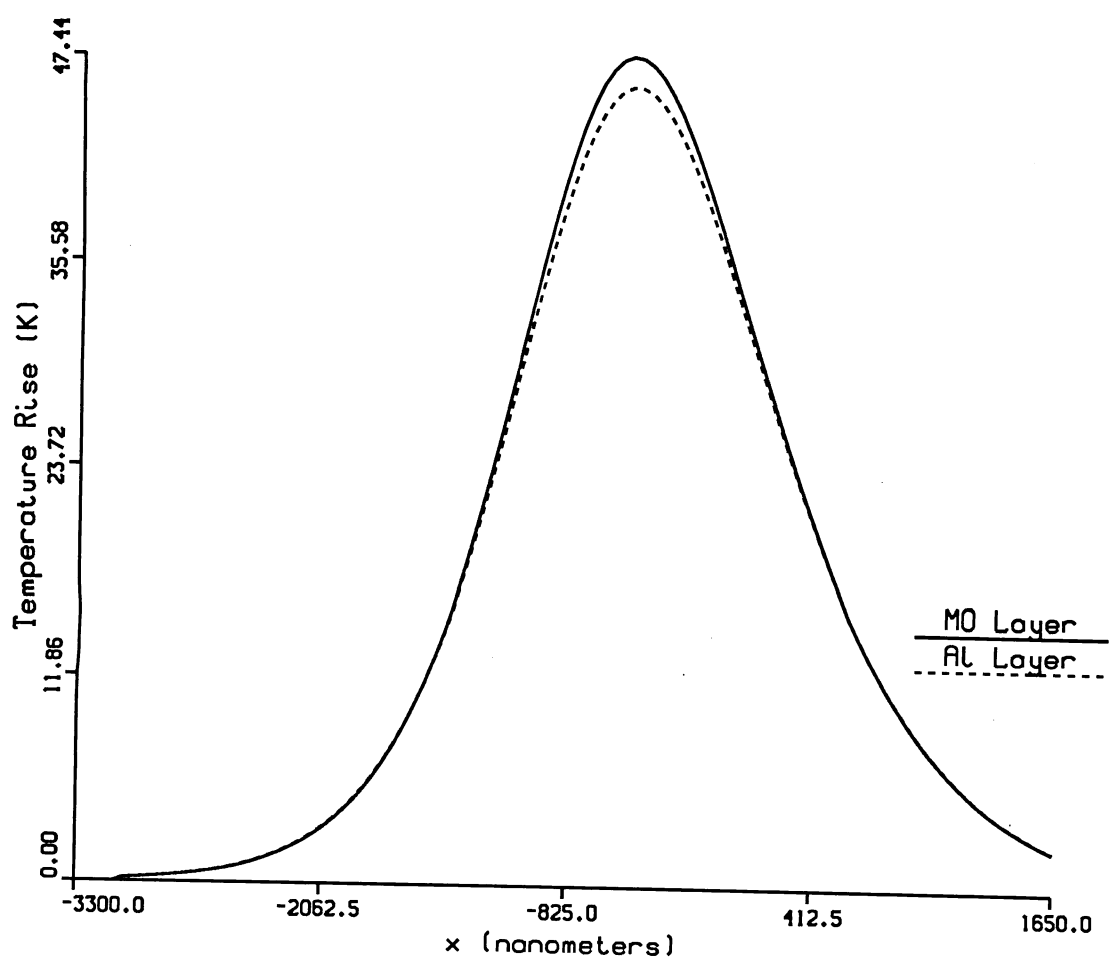


Figure 5

Temperature Rise at Spot Center vs X

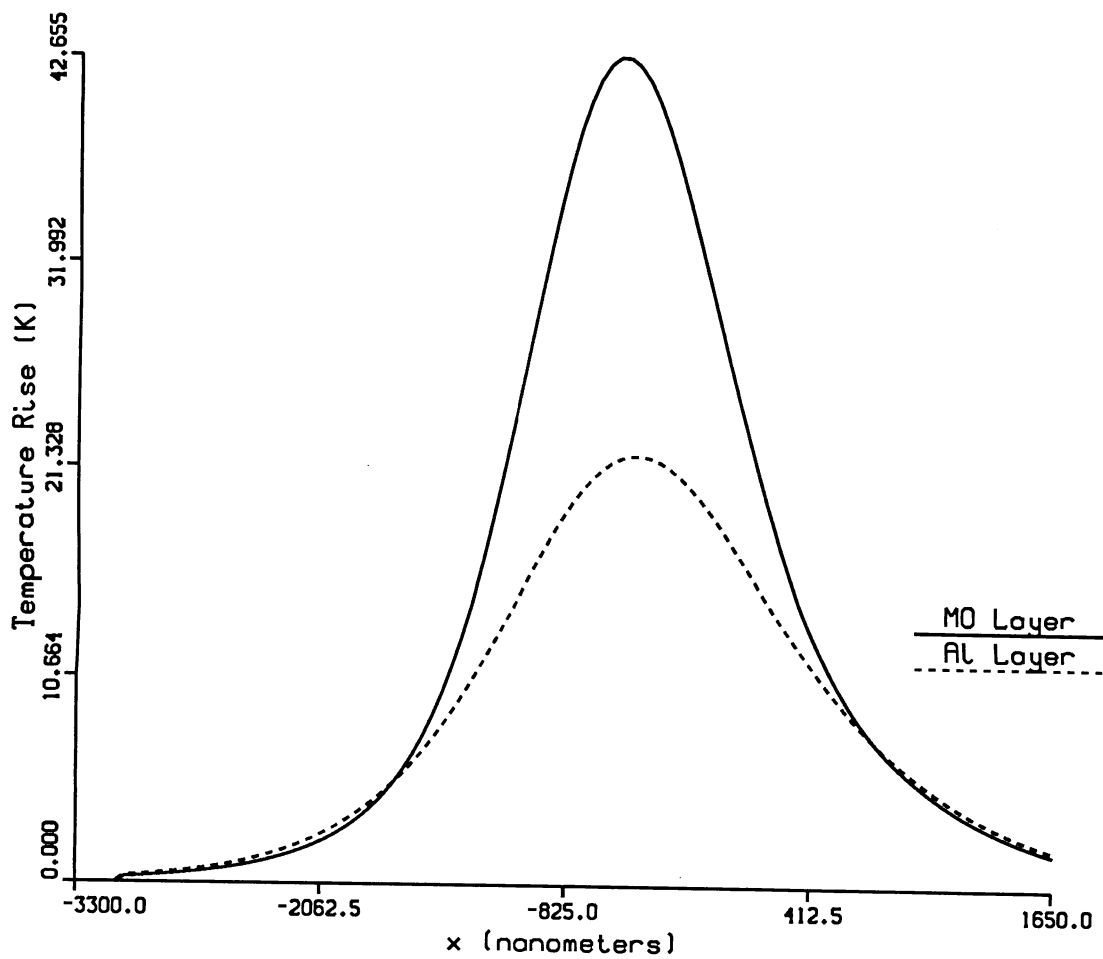


Figure 6